

# Computational investigation of pulsatile blood flow through sinusoidal stenoses of varying lengths

Md. Abdul Karim Miah\*, Ifat Rabbil Qudrat Ovi, Nasimul Eshan Chowdhury, Shorab Hossain, and Md. Nurul Absar Chowdhury

**Abstract**—Numerical simulations have been performed for two dimensional axisymmetric, laminar, pulsatile flow through modelled, sinusoidal stenosis with a mean Reynolds number of 578 with a maximum of 938 and minimum of 328. Blood has been considered as the Newtonian fluid. Investigations have been carried out for different lengths of the sine curve forming the stenosis shape and compared for the same severity of 56%. Input sinusoidal pulse of 2.9 Hz, corresponding to 345 milliseconds of time period, has been applied. Womersley number of 7.75 has been considered in the flow. Radial velocity distribution, vorticity and wall shear stress (WSS) distribution have been taken as the key parameters for analyzing and comparing stenosis of varying lengths. It has been concluded for the considered sinusoidal shaped stenosis that with the decrease in the lengths of the stenosis the vorticity, wall shear stress etc. gets concentrated towards the center of the stenosis and the peak values get higher indicating high risk in stenosis with smaller lengths.

**Keywords**—Stenosis, vorticity, Womersley Number ( $W_0$ ), Wall shear stress (WSS).

## I. INTRODUCTION

Over the last few decades, the role of fluid mechanics in the analysis of cardiovascular diseases has been great. Atherosclerosis occurs because of the deposition of lipids and accumulation of macrophages beneath the endothelial layer of the artery. And, due to the deposition of these materials beneath the endothelial layers, the flow area for the blood reduces leading to the increase velocity and pressure inside the artery [1]. Arterial stenosis is an abnormal narrowing of one of the arteries, as defined by the national institute of neurological disorders and stroke. Numerous researches on the hemodynamic characteristics of flow through the stenotic artery were carried out [2]–[4]. Presence of stenosis in an artery increases the risk for stroke as it causes the reduction of blood flow. The heart then needs to squeeze (contract) harder to pump blood.

Recent times, medical researchers, bioengineers and other scientists are giving their efforts to analyze the hemodynamic conditions using numerical simulation technique [5]. The main objective of blood flow simulation through arteries is to

investigate hemodynamic forces which artery wall experiences due to different factors- the pulsatile blood flow, the fluid flow geometry and the blood rheology behavior. Moreover, it is important to observe if there is any observable correlation between flow pattern characteristics and abnormal biological events and arterial diseases.

Considerable evidences have been found that vascular fluid dynamics play an important role in the development and progression of arterial stenosis [6]. So many researchers have done experiments and used CFD analysis to find out the flow disturbances caused because of the formation of stenosis in human being that leads to the failure of cardiovascular system [7]–[11]. After so many researches it has been proved that hemodynamic parameters play fundamental roles in regulating vascular biology and also in accessing of arterial diseases [12]. Hemodynamic parameters -wall shear stress, arterial wall strain, particle residence time and recirculation zones-are the most important out of all for investigating the flow behavior.

Several numerical and experimental works have been done to observe the blood flow behaviors using stenosis models considering the flow as pulsatile using both 2D and 3D approach and also using rigid and flexible wall [13], [14].

Ojha et al. [15] carried out investigation to find the flow behavior through arterial stenosis experimentally. Photochromic tracer method was used to find out the velocity profile of pulsatile flow at three axial locations in a flow channel. 2.9 Hz sinusoidal flow was used in the experiment and different degrees of severity were used. Mittal et al. [16] investigated pulsatile blood flow through modeled arterial stenosis having 50% semicircular constriction. It was found that the flow downstream of the stenosis exhibited all the classic features of post-stenotic flow. Turk et al. [17] studied the behavior of the bio fluid using magnetic source and stenosis. Stenoses of 40% and 60% severity were placed under magnetic source. And, it was found that flow is affected by the presence of both stenosis and magnetic field. Ikbal et al. [18] also carried out investigation using a rheology of blood using generalized Power law model. Razavi et al. [19] computed hemodynamic wall parameters at three Womersley numbers and it was found that the time-averaged reattachment point is maximum for the Newtonian model and minimum for the Power law model. Hasan et al. [20] studied the stenosis by varying different parameters. The effect of pulsation, stenosis size, Reynolds Number and Womersley number was observed for the laminar flow through a model of arterial stenosis. Feng et al. [21] conducted simulations of the blood flow through constricted tubes representing blood vessels with various degrees of steno-

\*Corresponding author.

Md. Abdul Karim Miah\*, Ifat Rabbil Qudrat Ovi, Nasimul Eshan Chowdhury, and Md. Nurul Absar Chowdhury are with the Department of Mechanical and Chemical Engineering, Islamic University of Technology, Dhaka, Bangladesh. e-mail: akarim2164@gmail.com, irqudrat@iut-dhaka.edu, nasimulikhlas@gmail.com and nabsar@iut-dhaka.edu

Shorab Hossain is with the Department of Engineering, BGMEA University of Fashion and Technology, Uttara, Dhaka, Bangladesh. e-mail: shorab@iut-dhaka.edu

Manuscript received June 16, 2018; revised November 10, 2018; Accepted December 02, 2018.

sis. They used very low Reynolds number (25-33) and found typical recirculation zones distal to the stenoses. Ishikawa et al. [22] analyzed periodic blood flow through a stenosed tube using numerical simulation. It was found that non-Newtonian property reduces the strength of the vortex downstream of stenosis and it has considerable influence on the flow as well. Ali et al. [23] presented a mathematical study for unsteady pulsatile flow of blood through using a tapered stenotic artery. The constitutive equation for Sisko model given in [23] is used to illustrate the rheology of blood. The axial velocity of blood, resistance to flow, flow rate and wall shear were found to be significantly influenced by the factors- blood rheology wall movement, presence of stenosis and degree of taperness of the artery.

Considerable amount of works have been done to observe the variation of different parameters in the blood flow in different modeled stenosis. Experiments and simulations for different degrees of severity are the very common researches. Effect of Womersley number (effect of pulsation) on the flow field, Effect of different blood rheology models to predict the blood flow, effect of varying Reynolds number on flow field, effect of Newtonian and Non-Newtonian behavior of blood on the flow field, effect of steady and pulsating modes of flow on flow parameters etc are notable researches carried out. However, to the best of author's knowledge, no studies have been attempted to investigate the effect of varying length of a sinusoidal stenosis with a fixed severity (depth). In this numerical modeling, the blood flow behavior using a sinusoidal stenosis of the varying length (period of sinusoid) has been studied to investigate the effects of laminar sinusoidal flow through the modeled stenotic artery.

## II. MATHEMATICAL MODELING

Simulations have been carried out with many assumptions which do not completely agree with physical phenomenon. Physical models considered have been moderated from realistic artery. Flow considered is sinusoidal but in real case flow is not as smooth as used in the simulation. Newtonian assumptions have been made despite the fact that blood is non-Newtonian.

General continuity and Navier-Stokes equation for the fluid flow is reduced for axisymmetric flow of incompressible, Newtonian fluids.

Continuity equation for incompressible flow in axisymmetric, cylindrical co-ordinate  $(r, X)$  can be written as:

$$\frac{1}{r} \frac{\partial(ru_r)}{\partial r} + \frac{\partial(u_x)}{\partial x} = 0$$

For incompressible flow in axisymmetric cylindrical co-ordinate  $(r, X)$ , the Navier-Stokes equations, neglecting body forces, are as follows.

Momentum in r direction:

$$\frac{\partial u_r}{\partial t} + u_r \frac{\partial u_r}{\partial r} + u_x \frac{\partial u_r}{\partial x} = -\frac{1}{\rho} \frac{\partial p}{\partial r} + \frac{\mu}{\rho} \left[ \frac{\partial}{\partial r} \left( \frac{1}{r} \frac{\partial(ru_r)}{\partial r} \right) + \frac{\partial^2 u_r}{\partial x^2} \right]$$

Momentum in X-direction:

$$\frac{\partial u_x}{\partial t} + u_r \frac{\partial u_x}{\partial r} + u_x \frac{\partial u_x}{\partial x} = -\frac{1}{\rho} \frac{\partial p}{\partial x} + \frac{\mu}{\rho} \left[ \frac{1}{r} \frac{\partial}{\partial r} \left( r \frac{\partial u_x}{\partial r} \right) + \frac{\partial^2 u_x}{\partial x^2} \right]$$

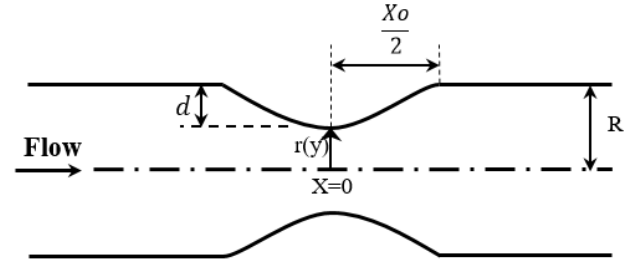


Fig. 1: Stenosis model used for present the simulation.

Here,  $r$  = radial co-ordinate,  $x$  = axial co-ordinate locating at the axis of the tube,  $u_r$  = velocity in radial direction,  $u_x$  = velocity in axial direction,  $p$  = pressure,  $\rho$  = density,  $\mu$  = dynamic viscosity.

## III. PHYSICAL MODEL

The schematic of local stenosis and some biological information are shown in Figure 01. As shown in this figure, a stenosis has been presented in the form of smooth sinusoidal or exponential profiles as taken from MODARES et al. [19].

$$r(y) = \begin{cases} R - \frac{d}{2} [1 + \cos(\frac{2\pi X}{X_0})], & \text{when } |x| \leq \frac{X_0}{2} \\ R, & \text{when } |x| > \frac{X_0}{2} \end{cases}$$

$r(y)$  = distance of the artery wall from the artery axis,  $R$  = unaffected artery Radius,  $X_0$  = Stenosis Length (period of the cosine curve),  $X$  = axial length from the center of the stenosis, and  $d$  = thickness of the stenosis.

## IV. GRID INDEPENDENCE TEST OF STENOSIS

Numerical results are required to be independent of the inlet and outlet lengths of the artery from the stenosis. Several numerical computations have been carried out to find the safe lengths so that the results become independent of the inlet and outlet lengths. And, it was found that 40 times and 60 times of the diameter lengths are appropriate to choose. Again, the grid is supposed to be such that the results will not show any variation with the change of the number of the cells. For the present simulation, the chosen grid shape was structured 2D mesh as shown in figure, and different optimized elements for different stenosis grids were: 38142, 47412, 48564 for  $L=1.6D$ ,  $2.4D$ ,  $3.2D$  respectively. The computational results, maximum WSS, with structured grid have been shown in the figure 2.

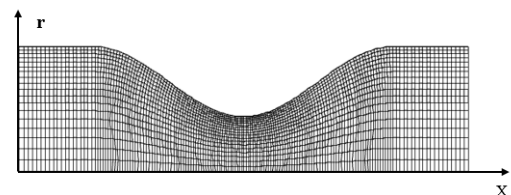


Fig. 2: structured grid of stenosis used for present simulation

TABLE I: Grid independency test for stenosis models

$X_0 = 1.6D$		$X_0 = 2.4D$		$X_0 = 3.2D$	
Elements (x1000)	Peak WSS (Pa)	Elements (x1000)	Peak WSS (Pa)	Elements (x1000)	Peak WSS (Pa)
11.736	40	11.852	29	12.14	19
17.604	53	17.776	36	18.21	21
23.34	57	23.702	43	24.278	35
29.34	60	29.628	48.57	30.348	42.5
38.142	61	38.52	48.5	39.448	42
46.944	61	47.412	49	48.564	42
55.746	61	56.29	49	57.664	42
64.548	61	65.178	49	66.76	42

## V. BOUNDARY CONDITIONS IN THE PRESENT COMPUTATION

Present simulation has been performed using frequency of 2.9 Hz with a mean flow rate of 4.3 ml/s having a fluctuation of 2.6 ml/s as used by [15], [19], [20]. Two parameters - fluid density of 0.755 g/cm<sup>3</sup> and viscosity of 1.43 cP have been used. Mean Reynolds number of 778 has been taken with a womersley number of 7.75. The boundary conditions used in the present simulation are given below.

### A. At Inlet

At the inlet of the computational domain, 'velocity inlet' boundary condition is used. The same sinusoidal volume flow as in Ojha et al. [15] shown in figure 4 is used but with a phase shift of 1280 (123 milliseconds). The velocity is found out by dividing the volume flow rate with the area.

$$Q = 4.3 + 2.6 \sin\left(\frac{2\pi t}{T}\right)$$

$$v_{inlet} = \frac{Q}{Area}$$

### B. At Outlet

At the outlet, the flow is considered fully developed. Zero normal gradient for all flow variables except pressure is considered as well. 'Outflow' boundary condition satisfies the following equation.

$$\frac{\partial u_r}{\partial x} = \frac{\partial u_x}{\partial x} = 0$$

### C. At centerline

In the computational domain, x axis has been considered as the axial symmetry condition.

### D. At wall

No slip boundary with no flow ( $u_x = u_r = 0$ ) is assumed at the wall section of the computational domain.

## VI. VALIDATION OF CFD CODE

To make the present simulation code acceptable, one previous, related published work was simulated and the results were compared with the results of the author. Our present code has been used to simulate the work of Ojha et al. [15]. They carried out experiments with the pulsatile, laminar flow which is same as the present one. Their model is shown in figure 03 where,  $\theta_1 = 30^\circ$  and  $\theta_2 = 45^\circ$ ,  $D=5\text{mm}$  and  $L=1.5\text{mm}$ . The centerline velocity distributions at the distal side of the stenosis at three normalized distance (with respect to diameter) of 1, 2.5 and 4.3 have been compared with that of Ojha et al. [15]. The pulsatile flow that they used had a frequency of 2.9 Hz, and, they used a mean flow rate of 4.3 ml/s having a fluctuation of 2.6 ml/s. The present simulation used the 'velocity inlet' as the flow inlet condition and the velocity used were found by dividing the flow rate of Ojha et al. [15] with the unrestricted area of the artery. Two parameters - fluid density of .755 g/cm<sup>3</sup> and viscosity of 1.43 cP have been used. The Newtonian assumption of the fluid has been considered. Mean Reynolds number of 778 has been taken with a womersley number of 7.75. Volumetric flow rate as used by Ojha et al. [15] has been shown in figure 4.

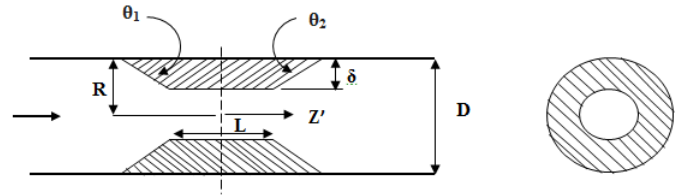


Fig. 3: Geometry of the stenosis used by Ojha et al. [15], where  $L$ =length at the end portion,  $D$ = diameter of the unaffected tube,  $\delta$ =depth of stenosis,  $Z' = Z/D$  (normalized distance from the center of the models on the right side is the cross sectional view of models)

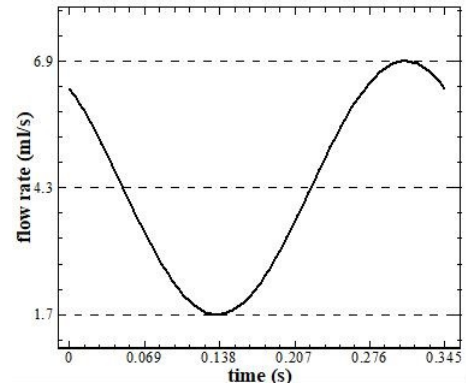
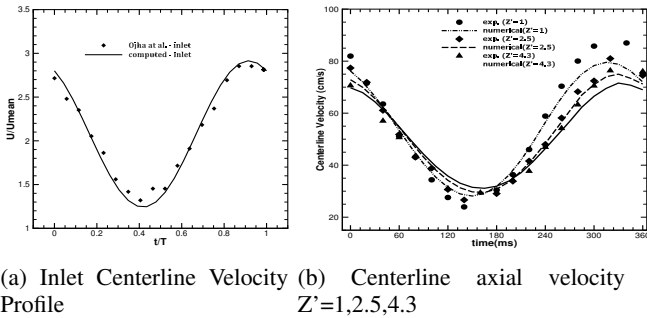


Fig. 4: Volumetric flow at the inlet of the artery used by Ojha et al. [15]

The velocity at the inlet has been compared first in figure 5a. It can be seen that velocities are similar throughout except at the beginning and the end portion. This little difference in the

velocity causes discrepancy in the experimental and simulated results.

The experimental time varying velocity at different distal areas are lower for higher lengths of the stenosis. So, velocity tends to increase for the higher lengths of the stenosis as, with the decrease of the flow area, the velocity increases. For stenosis lengths of 1.6D, 2.4D and 3.2D, the centerline velocities are 4.28, 5.55 and 6.6 times of the mean velocity. At  $X=-0.8D$ , the cross section areas are slight lower for higher lengths of stenosis. At this section, for stenosis lengths of 1.6D, 2.4D and 3.2D, the centerline velocities are 2.8, 3.2 and 3.96 times of the mean velocity. And, at  $X=-1.2D$ , the cross section areas are almost equal for stenosis of different lengths. So, the velocity profiles are almost similar.



(a) Inlet Centerline Velocity Profile (b) Centerline axial velocity at  $Z'=1,2,5,4,3$

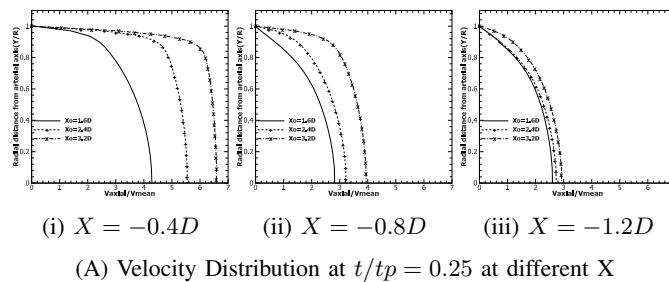
Fig. 5: Validation from Ojha et al. (a) Inlet Centerline Velocity Profile (b) Centerline axial velocity at  $Z'=1,2,5,4,3$

## VII. RESULTS AND DISCUSSIONS

### A. Radial velocity distribution and contour

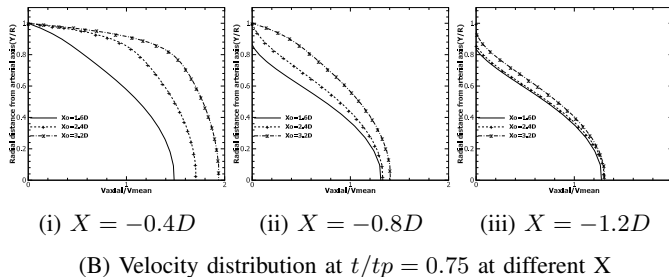
The flow parameters, because of the presence of the stenosis, varies more significantly, for varying lengths of the stenosis, at the pre-stenotic regions than at the post stenotic regions. So, the velocity profiles at different pre-stenotic regions have been chosen for comparison.

In figure 6A, velocity profiles, at  $t/tp = .25$  when flow is accelerating, of the flow through stenosis of different lengths are shown at different pre-stenotic positions - at a distance of



(i)  $X = -0.4D$  (ii)  $X = -0.8D$  (iii)  $X = -1.2D$

(A) Velocity Distribution at  $t/tp = 0.25$  at different X



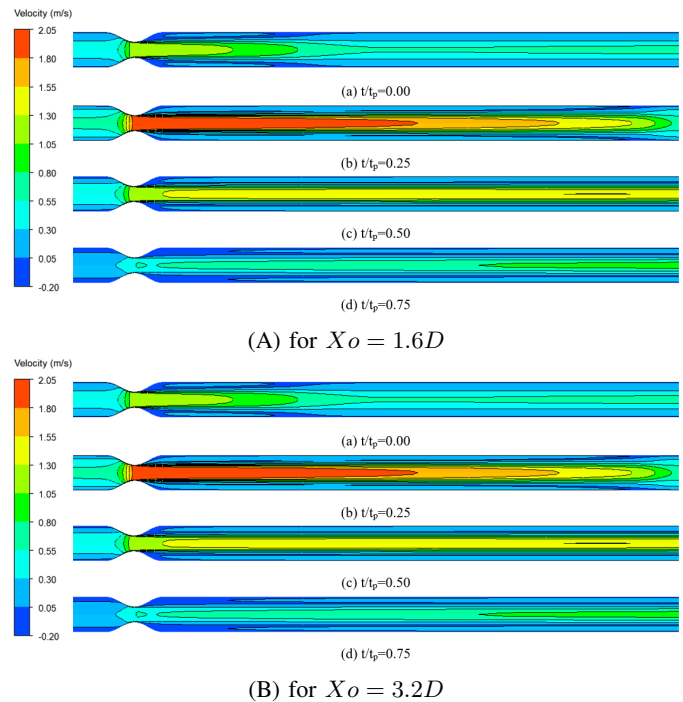
(i)  $X = -0.4D$  (ii)  $X = -0.8D$  (iii)  $X = -1.2D$

(B) Velocity distribution at  $t/tp = 0.75$  at different X

Fig. 6: Velocity Distribution in radial direction at (A)  $t/tp = .25$  and (B)  $t/tp = .75$  for at  $X = -0.4D, -0.8D$  and  $-1.2D$  in the pre-stenotic region

0.4D, 0.8D and 1.2D from the centre of the throat. At  $X=-0.4D$ , very close to the centre of the throat, the cross section areas are lower for higher lengths of the stenosis. So, velocity tends to increase for the higher lengths of the stenosis as, with the decrease of the flow area, the velocity increases. For stenosis lengths of 1.6D, 2.4D and 3.2D, the centerline velocities are 4.28, 5.55 and 6.6 times of the mean velocity. At  $X=-0.8D$ , the cross section areas are slight lower for higher lengths of stenosis. At this section, for stenosis lengths of 1.6D, 2.4D and 3.2D, the centerline velocities are 2.8, 3.2 and 3.96 times of the mean velocity. And, at  $X=-1.2D$ , the cross section areas are almost equal for stenosis of different lengths. So, the velocity profiles are almost similar.

In figure 6B, velocity profiles have been shown for  $t/tp = .75$  when flow is decelerating. The centerline velocities are much less than that at  $t/tp = .25$ . For stenosis lengths of 1.6D, 2.4D and 3.2D, the centerline velocities are 1.48, 1.68 and 1.95 times of the mean velocity. At  $X=-0.8D$ , for stenosis lengths of 1.6D, 2.4D and 3.2D, the centerline velocities are 1.305, 1.32 and 1.405 times of the mean velocity.



(A) for  $Xo = 1.6D$

(B) for  $Xo = 3.2D$

Fig. 7: Velocity Contours at four key points for (A)  $Xo = 1.6D$  and (B)  $Xo = 3.2D$

In figure 7, the velocity contour, mostly of the post-stenotic region, have been shown both for stenosis lengths of  $Xo=1.6D$  and  $Xo=3.2D$  for comparison. In the figure it is evident that, for both of the stenosis lengths, the contours do not differ significantly except that there are little changes of magnitudes of few parameters. In both of the cases, the velocity magnitudes are maximum for  $t/tp=0.25$  when the flow is accelerating. And it is slightly lower for  $t/tp=0.50$ . And, the magnitudes are lowest for  $t/tp=0.75$  when the flow is decelerating. The recirculation region is thicker for the stenosis length of 1.6 than for the stenosis length of 3.2D. For the stenosis length of 1.6D, the flow is suddenly exposed at the post-stenotic

region because of sudden increase of area. Compared to this, for stenosis length of 3.2D, the flow is gradually exposed at the post-stenotic region because of the gradual increase of the area.

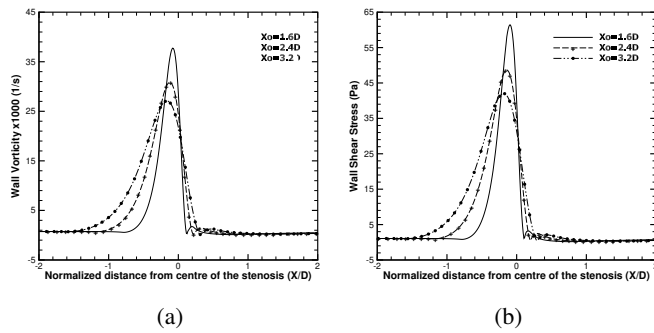


Fig. 8: (a)Wall vorticity and (b)Wall shear stress distribution for different stenosis Lengths ( $X_o=1.6D, 2.4D$  and  $3.2D$ ) at  $t/tp=0.25$

Vorticity is the microscopic measure of the rotation of a fluid element at any point (defined as the curl of velocity vector). This is another parameter by which the disturbance (in the form of microscopic rotation that is induced) created in a flow because of the presence of stenosis can be observed. In figure 8a, the wall vorticity that is produced for different stenosis lengths are shown at  $t/tp=0.25$  when flow is accelerating. It is seen that vorticity influence is high and is distributed along a higher length in the pre-stenotic region. The peak wall vorticity is maximum for minimum stenosis lengths. And, the vorticity decreases for increase of the stenosis length. For the lower stenosis length, the vorticity increases abruptly near the throat of the stenosis and it is induced because of abrupt change of the velocity components near the stenosis. The abrupt change area accounts for the abrupt change of velocity component. However, for higher stenosis length, the gradual change of the area induces vorticity but the peak vorticity is low, as the disturbance is gradually distributed along the higher length of the stenosis.

Wall shear stress is the most important parameter to observe the risk of the wall rupture. In figure 8b, the wall shear stress distribution for different stenosis lengths are shown for the time when flow is accelerating that is at  $t/tp = 0.25$ , the wall shear stress distribution covers maximum lengths in the pre-stenotic region. Because the flow is contracted suddenly in the pre-stenotic region with the higher velocity gradient (observed in figure 6), it induces shear which ultimately results in the wall shear stress. For lower stenosis length, the wall shear is concentrated toward the center of the stenosis and peak wall shear is the higher compared to the any higher stenosis lengths. In case of higher stenosis lengths, the induced wall shear stress is distributed along the lengths of the stenosis and peak wall shear stress is not that high as compared to that of stenosis of lower lengths.

### VIII. CONCLUSION

At present study, sinusoidal stenosis with severity of 56% has been considered where the period of the sinusoid is the

length of the stenosis. Flow was laminar with mean Reynolds number of 578 having a frequency of 2.9 Hz (corresponding to time period of 345 milliseconds). Using different lengths of stenosis, the following observations have been made.

- The variation of the stenosis length causes the parameter variation mostly in the pre-stenotic region.
- Lower stenosis length causes thicker recirculation region in the post stenotic region
- Lower stenosis length causes concentrated wall vorticity towards the center of the stenosis and lower stenosis length induces higher peak wall vorticity
- Same as vorticity, lower stenosis length causes concentrated wall shear stress towards the center of the stenosis. With the decrease of the stenosis length, the peak wall shear stress increase.

Based on the observations, for the sinusoidal curved stenosis of the same severity, stenosis of lower length causes maximum and abrupt disturbance in the flow. So, the stenosis of lower lengths are highly risky compared to that of lower length.

### REFERENCES

- [1] N. Nandakumar and M. Anand, "Pulsatile flow of blood through a 2d double-stenosed channel: effect of stenosis and pulsatility on wall shear stress," *International Journal of Advances in Engineering Sciences and Applied Mathematics*, vol. 8, no. 1, pp. 61–69, 2016.
- [2] W. Choi, S. H. Park, H. K. Huh, and S. J. Lee, "Hemodynamic characteristics of flow around a deformable stenosis," *Journal of Biomechanics*, vol. 61, pp. 216–223, 2017.
- [3] C. Pagiatakis, J.-C. Tardif, P. L. L'Allier, and R. Mongrain, "A numerical investigation of the functionality of coronary bifurcation lesions with respect to lesion configuration and stenosis severity," *Journal of Biomechanics*, vol. 48, no. 12, pp. 3103–3111, 2015.
- [4] S. Sankaran, H. J. Kim, G. Choi, and C. A. Taylor, "Uncertainty quantification in coronary blood flow simulations: impact of geometry, boundary conditions and blood viscosity," *Journal of biomechanics*, vol. 49, no. 12, pp. 2540–2547, 2016.
- [5] M. N. Uddin and M. Alim, "Numerical study of blood flow through symmetry and non-symmetric stenosis artery under various flow rates," *IOSR Journal of Dental and Medical Sciences*, vol. 16, no. 6, pp. 106–115, 2017.
- [6] C. Tu and M. Deville, "Pulsatile flow of non-newtonian fluids through arterial stenoses," *Journal of biomechanics*, vol. 29, no. 7, pp. 899–908, 1996.
- [7] P. Blanco, L. Müller, S. Watanabe, and R. Feijóo, "Computational modeling of blood flow steal phenomena caused by subclavian stenoses," *Journal of Biomechanics*, vol. 49, no. 9, pp. 1593–1600, 2016.
- [8] V. Deplano, Y. Knapp, L. Bailly, and E. Bertrand, "Flow of a blood analogue fluid in a compliant abdominal aortic aneurysm model: Experimental modelling," *Journal of Biomechanics*, vol. 47, no. 6, pp. 1262–1269, 2014.
- [9] Y. Imai, T. Omori, Y. Shimogonya, T. Yamaguchi, and T. Ishikawa, "Numerical methods for simulating blood flow at macro, micro, and multi scales," *Journal of biomechanics*, vol. 49, no. 11, pp. 2221–2228, 2016.
- [10] P. Reorowicz, D. Obidowski, P. Klosinski, W. Szubert, L. Stefanczyk, and K. Jozwik, "Numerical simulations of the blood flow in the patient-specific arterial cerebral circle region," *Journal of biomechanics*, vol. 47, no. 7, pp. 1642–1651, 2014.
- [11] S. S. Khalafvand, E. Y.-K. Ng, L. Zhong, and T.-K. Hung, "Three-dimensional diastolic blood flow in the left ventricle," *Journal of Biomechanics*, vol. 50, pp. 71–76, 2017.
- [12] J. R. Buchanan Jr, C. Kleinstreuer, G. A. Truskey, and M. Lei, "Relation between non-uniform hemodynamics and sites of altered permeability and lesion growth at the rabbit aorto-celiac junction," *Atherosclerosis*, vol. 143, no. 1, pp. 27–40, 1999.
- [13] J. Janela, A. Moura, and A. Sequeira, "A 3d non-newtonian fluid-structure interaction model for blood flow in arteries," *Journal of Computational and Applied Mathematics*, vol. 234, no. 9, pp. 2783–2791, 2010.

- [14] V. Chabannes, G. Pena, and C. Prud'Homme, "High-order fluid-structure interaction in 2d and 3d application to blood flow in arteries," *Journal of Computational and Applied Mathematics*, vol. 246, pp. 1–9, 2013.
- [15] M. Ojha, R. S. Cobbold, K. W. Johnston, and R. L. Hummel, "Pulsatile flow through constricted tubes: an experimental investigation using photochromic tracer methods," *Journal of fluid mechanics*, vol. 203, pp. 173–197, 1989.
- [16] R. Mittal, S. Simmons, and H. Udaykumar, "Application of large-eddy simulation to the study of pulsatile flow in a modeled arterial stenosis," *Journal of biomechanical engineering*, vol. 123, no. 4, pp. 325–332, 2001.
- [17] Ö. Türk, M. Tezer-Sezgin, and C. Bozkaya, "Finite element study of biomagnetic fluid flow in a symmetrically stenosed channel," *Journal of Computational and Applied Mathematics*, vol. 259, pp. 760–770, 2014.
- [18] M. A. Iqbal, S. Chakravarty, K. K. Wong, J. Mazumdar, and P. K. Mandal, "Unsteady response of non-newtonian blood flow through a stenosed artery in magnetic field," *Journal of Computational and Applied Mathematics*, vol. 230, no. 1, pp. 243–259, 2009.
- [19] M. M. Razavi, S. Seyedein, and P. Shahabi, "Numerical study of hemodynamic wall parameters on pulsatile flow through arterial stenosis," *IUST International Journal of Engineering Science*, vol. 17, no. 3-4, pp. 37–46, 2006.
- [20] A. T. Hasan and D. D. Kanti, "Numerical simulation of sinusoidal fluctuated pulsatile laminar flow through stenotic artery," *Journal of Applied Fluid Mechanics*, vol. 1, no. 2, pp. 25–35, 2008.
- [21] R. Feng, M. Xenos, G. Girdhar, W. Kang, J. W. Davenport, Y. Deng, and D. Bluestein, "Viscous flow simulation in a stenosis model using discrete particle dynamics: a comparison between dpd and cfd," *Biomechanics and modeling in mechanobiology*, vol. 11, no. 1-2, pp. 119–129, 2012.
- [22] T. Ishikawa, S. Oshima, and R. Yamane, "Vortex enhancement in blood flow through stenosed and locally expanded tubes," *Fluid Dynamics Research*, vol. 26, no. 1, p. 35, 2000.
- [23] N. Ali, A. Zaman, and M. Sajid, "Unsteady blood flow through a tapered stenotic artery using sisko model," *Computers & Fluids*, vol. 101, pp. 42–49, 2014.



**Nasimul Eshan Chowdhury** received his B.Sc. Engg. in Mechanical Engineering degree from Islamic University of Technology (IUT), Bangladesh in 2018. His research interests include CFD, Numerical Phase Change Modelling.



**Shorab Hossain** received his B.Sc. in Mechanical Engineering degree from Islamic University of Technology (IUT), Bangladesh in 2015. Currently he is doing his M.Sc. in Mechanical Engineering in King Fahd University of Petroleum and Minerals (KFUPM), KSA. He worked as a Lecturer in Engineering Department, BGMEA University of Fashion and Technology (BUFT), Bangladesh. His research interest includes Combustion and Clean Energy, CFD, Biofluid. Thermal Desalination System.



**Md. Abdul Karim Miah** received his B.Sc. and M.Sc. in Mechanical Engineering degree from Islamic University of Technology (IUT), Bangladesh in 2014 and 2018 respectively. Currently he is working as a lecturer in the Department of Mechanical and Chemical Engineering(MCE), Islamic University of Technology (IUT), Bangladesh. His research interests include Bio Fluid, CFD.



**Ifat Rabbil Quadrat Ovi** received his B.Sc. Engg. in Mechanical Engineering degree from Islamic University of Technology (IUT), Bangladesh in 2014. Currently he is working as a lecturer in the Department of Mechanical and Chemical Engineering(MCE), Islamic University of Technology (IUT), Bangladesh and also pursuing his M.Sc. Engg. in Mechanical Engineering at the same university. His research interests include Arterial Blood Flow, CFD, Analysis and Control of Dynamic Systems.



**Md. Nurul Absar Chowdhury** received his Ph.D degree in Mechanical Engineering from Moscow State Auto-mechanical University, Russia in 1989. Currently he is working as a professor in the Department of Mechanical and Chemical and Engineering (MCE) in Islamic University of Technology (IUT), Bangladesh and also working as the Dean of Faculty of Engineering and Technology in the same university. His research interests include Parametric Machine design, Mathematical modeling and computer simulation of manufacturing Processes, automation and Computerization of Manufacturing System and Mechatronics in manufacturing process control.